

## Supplementary Information

### Electrochemically active surface area (EASA)

The accessible surface area of as-synthesized samples (M 150, M 500) could be approximated from the EASA. For this, the EASA was estimated from the double layer capacitance ( $C_{dl}$ ) via cyclic voltammetry (CV) measurement. CV was performed on an Autolab potentiostat/galvanostat electrochemical workstation (PGSTAT302N, The Netherlands) in a cell with three electrodes at ambient temperature. An Ag/AgCl (3 M KCL) electrode and a platinum electrode were used as the reference and counter electrode, respectively. The working electrodes were fabricated by depositing catalyst inks on a rectangular-shaped non-wet proofed carbon cloths (1×1 cm, type B-1A, E-TEK) using the drop-drying method at ambient temperature. The catalyst inks were prepared by sonicating as-synthesized samples (M 150, M 500) for 10 min in an isopropyl alcohol and 15 wt% Nafion. Prior to deposition, the carbon clothes were sequentially cleaned in acetone, 1M HCl solution, deionized water, and ethanol under sonication for 15 min each, and then dried. The sample loaded carbon clothes were compressed prior to CV measurements. The mass of M 150 and M 500 catalysts was about 0.51 and 0.36 mg on the carbon cloths, respectively. This was determined by measuring the weight of carbon cloths before and after MnO<sub>2</sub> nanomaterial loading. The electrolyte was 0.5 M aqueous Na<sub>2</sub>SO<sub>4</sub> solution. The CV measurements were repeated three times with a new working electrode each time. There was a very good reproducibility of the as-prepared working electrode. Thus, the EASA was estimated according to the equation  $EASA=C_{dl}/C_s$ . The CV curves in a non-faradaic region (-0.3 to 0.3 V) were plotted as a function of various scan rates (20, 30, 40, 50, 60, 80, 90 mV/s) (Fig. S1a and b). Then, the double layer capacitance ( $C_{dl}$ ) was assessed from the slope of the linear regression between the current density differences ( $\Delta j/2 = (j_a-j_c)/2$ ) in the middle of the potential window of CV curves versus the scan rates (Fig. S1c).  $C_s$  stands for the specific

capacitance of standard electrode materials on a unit surface area. Here, based on the literature reported  $C_s$  values for carbon electrode materials,  $0.02 \text{ mF/cm}^2$  was considered for EASA calculation.<sup>1-4</sup> The EASA was converted from  $\text{cm}^2$  to  $\text{m}^2/\text{g}$  by dividing the ECSA area by the mass loading of catalysts.

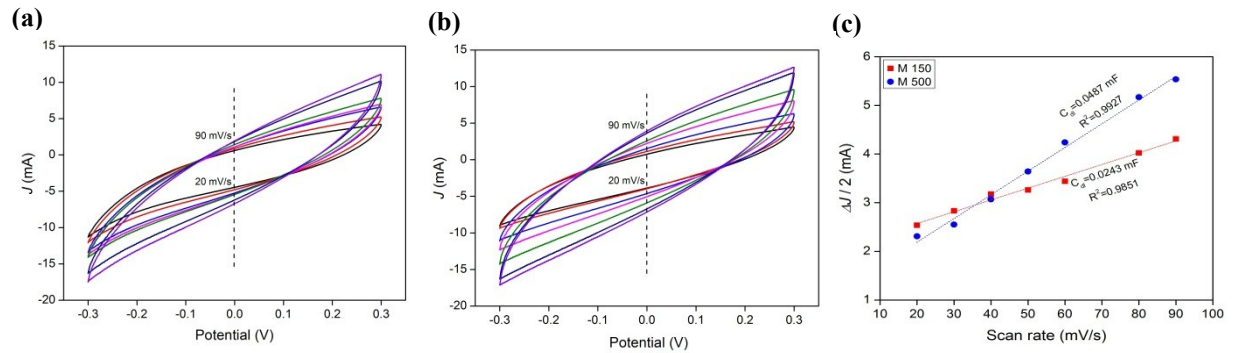


Fig. S1. CV curves in a non-faradaic region (-0.3 to 0.3 V vs. Ag/AgCl) at scan rates of 20, 30, 40, 50, 60, 80, 90 mV/s for (a) M 150 and (b) M 500 samples, and (c) linear regression between the current density differences in the middle of the potential window of CV vs. scan rates for M 150 and M 500 samples.

### Electrochemical analysis of MFCs

The electrochemical traits (CV and EIS) of the MFCs (M 500-DL and Pt/C MFCs) were investigated under stable open circuit voltage (when adequate substrate was available) with an Autolab potentiostat (PGSTAT302N, The Netherlands). The working electrode was linked to the anode and combined reference/counter electrode was linked to the cathode. CV was conducted at  $10 \text{ mV/s}$  between a potential range of  $1$  and  $-1 \text{ V}$ . The absolute area under

the CV curves was determined according to the equation 
$$AUC = \int_{V_1}^{V_2} I(V) dV$$
, where AUC

stands for the absolute area under the curve (I.V),  $V_2 - V_1$  stands for the potential range and I (V) stands for the response current (A). EIS test was performed with  $0.05 \text{ mV}$  amplitude and  $1 \text{ MHz} - 0.1 \text{ Hz}$  frequency limits.

As illustrated in Fig S2a, a visible redox peaks were observed in the CV of M 500-DL MFCs. The anodic peak is related to the presence of redox species in MFCs. In the Pt/C MFCs, no noticeable redox peaks were obtained during the CV tests. While, the current response was high (AUC = 9.40 I.V, limiting current = 6.01 mA). This represents the high catalytic activity of Pt/C and electrogenic activity of the microbial population in the MFCs. It has been reported that the unclear redox peaks basically does not mean no catalytic activity.<sup>5</sup> In fact, the high catalytic activity of Pt/C is due to its high surface area and electrical conductivity. This particularly causes a low charge transfer resistance in Pt/C MFCs (Fig S2b and c). The CV absolute area and limiting current was assessed to be 2.94 I.V and 4.31mA in M 500-DL MFCs, respectively. This was covering 31% of the AUC and lowering 28% limiting current evaluated in Pt/C MFCs.

From the conducted EIS tests (Fig. S2b), the Nyquist plots of the MFCs possess a high frequency semicircle and a low frequency straight line as a result of Warburg diffusion. The impedance data were analyzed by fitting the Nyquist plots. The intersection point between semicircles and real axis at high frequency region signifies the ohmic resistance ( $R_{ohm}$ ) of the MFCs. The diameter of the semicircles is proportional to the charge transfer resistance ( $R_{ct}$ ) at the electrode surface. The diffusion coefficient of the culture medium into the cathode electrode are determined according to the equation  $D = 0.5(RT/AF^2\sigma C)^2$ , where R stands for the gas constant (J/mol.K), T stands for the absolute temperature (K), A stands for the surface area of the cathode electrode (cm<sup>2</sup>), F stands for the Faraday's constant (amp.s/mol),  $\sigma$  stands for the slope of the straight lines signifies the values of the Warburg coefficient (ohm/s<sup>1/2</sup>), and C stands for the molar concentration of the PBS solution (mol/cm<sup>3</sup>).<sup>6</sup> The results showed that the Pt/C MFCs possess a higher ohmic resistance (18%) and lower diffusion coefficient (78%) than M 500-DL MFCs (Fig. S2c). This possibly is due to the thick biofilm formed on the cathodes.<sup>7, 8</sup> The ohmic resistance was estimated to be 36.60  $\Omega$  and 44.59  $\Omega$  in MFCs with

M 500-DL and Pt/C cathodes, respectively. In that order, diffusion coefficient was found to be  $3.13 \times 10^{-10} \text{ cm}^2 \cdot \text{s}^{-1}$  and  $0.69 \times 10^{-10} \text{ cm}^2 \cdot \text{s}^{-1}$ . Despite this, the MFCs with Pt/C cathode ( $20.72 \text{ } \Omega$ ) displayed a lower charge transfer resistance (40%) than M 500-DL MFCs ( $34.66 \text{ } \Omega$ ), possibly due to high surface area and electrical conductivity of Pt/C catalyst. This results in high performance in Pt/C MFCs (Fig. 7a and b). The CV and EIS analysis of MFCs equipped with M 500-DL and Pt/C cathodes were well suited to empirical data.

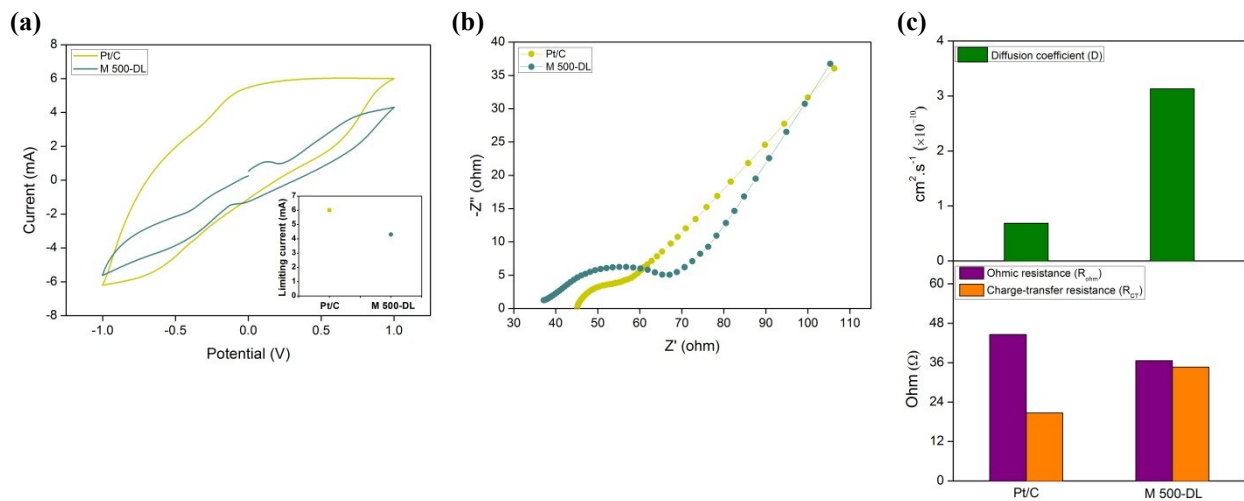


**Fig. S2** (a) Cyclic voltammety, (b) Nyquist impedance plots, and (c) related-impedance parameters of MFCs with M 500-DL and Pt/C cathodes.

### Effect of glucose on the performance of M 500-DL MFCs

Glucose is also one of the commonly used substrate in MFCs. After extensive experimentations on the acetate-fed MFCs with different cathode catalysts, the response of voltage generation to the substrate changes was particularly tested in the MFCs with M 500-DL cathode by suddenly changing the substrate to another type containing glucose (over a period of 17 days). As illustrated in Fig. S3a, after initial acclimatization, glucose-fed reproducible cycles of voltage generation were observed in the MFCs with a similar trend to those fed with acetate substrate (Fig. 6), but at a lower voltage output level (10%). They

sustained stable voltage for approximately 34 h. According to four batch cycles of operation, the mean stable voltage of glucose-fed MFCs reached  $272 \pm 0.44$  mV (at an external resistance of  $985 \Omega$ ). From the glucose-fed MFCs ( $555 \pm 8$  mV OCP) (Fig. S3b), the obtained maximum power density ( $154 \pm 7$  mW/m<sup>2</sup>,  $0.09 \pm 0.002$  mA/cm<sup>2</sup>) was lower (28%) than those fed with acetate (Fig. 7a). Furthermore, the low CE ( $10 \pm 1\%$ ) and the high internal resistance ( $257 \pm 5 \Omega$ ) was estimated in MFCs with the glucose culture medium. The low performance in the glucose-fed MFCs can explain by the reason that glucose could not directly consume by electrogenic bacteria. In fact, glucose is a substrate that can be fermented and metabolized in various competing routes, including fermentation and methanogenesis, which are unable to generate electricity.<sup>9</sup> The internal resistance in the glucose-fed MFCs increased due to the complexity of the substrate.<sup>10</sup>

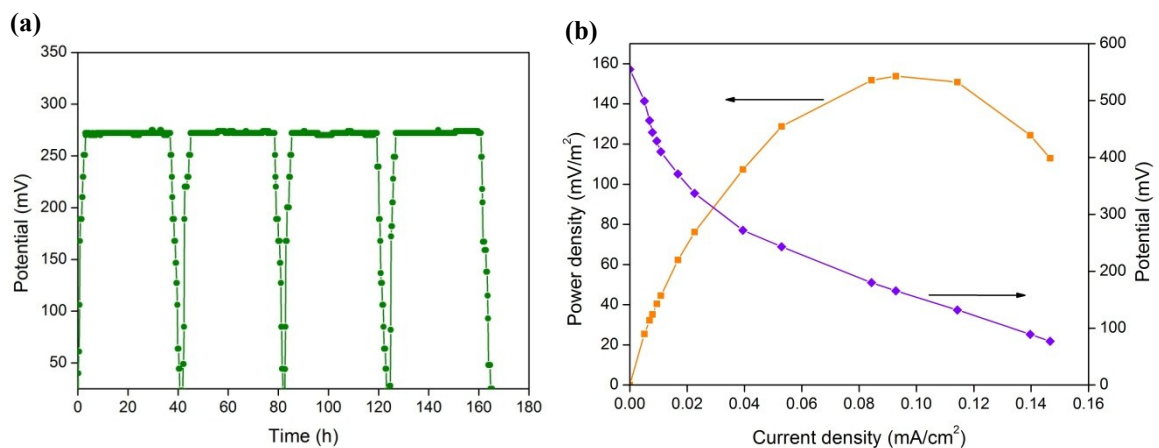


**Fig. S4** (a) Voltage generation (at an external resistance of  $985 \Omega$ ) and (b) power density and polarization curves of the M 500-DL MFCs fed with glucose culture media.

Table S1 Pre-estimated total capital cost of MFCs for 1 m<sup>3</sup> feed-substrate.

Compounds	MFCs	
	Pt/C	M 500-DL
Reactor volume (m <sup>3</sup> )	1	1
Anode electrode area (m <sup>2</sup> )	25	25
Cathode electrode area (m <sup>2</sup> )	25	25
Catalyst used (g)	1250	250
Reactor cost (plexiglass) (US\$)	1450	1450
Anode cost (US\$)	7029	7029
Catalyst cost (US\$)	60750	57
Carbon cloth (30% we proof)	14063	14063
Cathode cost (US\$)	74813	14120
Total cost (US\$)	83292	22599

## References

- 1 A. Kundu and T.S. Fisher, *Electrochim. Acta*, 2018, **281**, 357-369.
- 2 G. Xiong, P. He, Z. Lyu, T. Chen, B. Huang, L. Chen and T.S. Fisher, *Nat. Commun.*, 2018, **9**, 790-800.
- 3 S. Ghosh, B. Gupta, T. Mathews, A. Das, M. Kamruddin, *Nano Struct. Nano Objects*, 2017, **10**, 42-50.
- 4 S.K. Bikkarolla, P. Cumpson, P. Joseph and P. Pagona, *Faraday Discuss.*, 2014, **173**, 415-428.
- 5 L. Xiao, J. Damien, J. Luo, H.D. Jang, J. Huang and Z. He, *J. Power Sources*, 2012, **208**, 187-192.
- 6 Z. He, Z. Wang, Z. Huang, H. Chen, X. Li and H. Guo, *J. Mater. Chem. A*, 2015, **3**, 16817-16823.
- 7 S. Yang, B. Jia and H. Liu, *Bioresour. Technol.*, 2009, **100**, 1197-1202.
- 8 Y. Yuan, S. Zhou and J. Tang, *Environ. Sci. Technol.*, 2013, **47**, 4911-4917.
- 9 D. Pant, G. Van Bogaert, L. Diels and K. Vanbroekhoven, *Bioresour. Technol.*, 2010, **101**, 1533-1543.
- 10 S.B. Velasquez-Orta, E. Yu, K.P. Katuri, I.M. Head, T.P. Curtis and K. Scott, *Appl. Microbiol. Biotechnol.*, 2011, **90**, 789-798.